Detailed mapping of sand injectites integrating seismic attribute analysis and machine learning techniques in the Norwegian North Sea

Anna Rumyantseva[1]*, Jaswinder Mann-Kalil[1], Sara Mitchell[1], Dean Macaulay[1] and Alaa Triki[1],
illustrate a methodology for achieving detailed mapping of sand injectites in the Greater Fram area by using seismic attribute analysis and integrating machine learning (ML) techniques specifically designed for detecting injectites and faults.

Introduction

The Norwegian North Sea is an established oil and gas province where there continues to be sustained exploration and development efforts, with a focus on infrastructure-led exploration (ILX) strategies in recent years. Many discoveries within the remobilised sands of Paleocene and Eocene age have proven the injectite play. Large-scale sandstone intrusives have been actively explored in the South Viking Graben (SVG) since the first discovery in the Balder Field in 1967. Further north, in the North Viking Graben (NVG), the injectite play has recently been confirmed by discoveries such as Kveikje (2022) and Heisenberg (2023). For the 2024 exploration campaigns, operators have expressed interest in two new promising injectite prospects in the NVG area.

Recent advances in seismic imaging technology have significantly improved the understanding of the complex geometries of sand intrusions. This paper illustrates a robust methodology for achieving detailed mapping of sand injectites in the Greater Fram area (Figure 1), by using seismic attribute analysis, including RGB frequency blending from spectral decomposition analysis, and integrating machine learning (ML) techniques specifically designed for detecting injectites and faults. Combining these approaches enables a granular understanding of subsurface dynamics and facilitates enhanced reservoir characterisation. The key to our methodology is using newly processed dual-azimuth (DAZ) seismic data, characterised by advances in pre-processing, noise mitigation, and velocity model building (VMB) technologies. By leveraging reimaged north-south data with newly acquired east-west data we see uplifts in terms of illumination, resolution, signal-to-noise ratio, and demultiple (Buriola et al., 2023). Utilising ML to identify injectite geobodies provides deeper insights into these subsurface reservoirs, which allows a better understanding of the geometries of the injectites, and helps to increase the efficiency of hydrocarbon exploration and production.

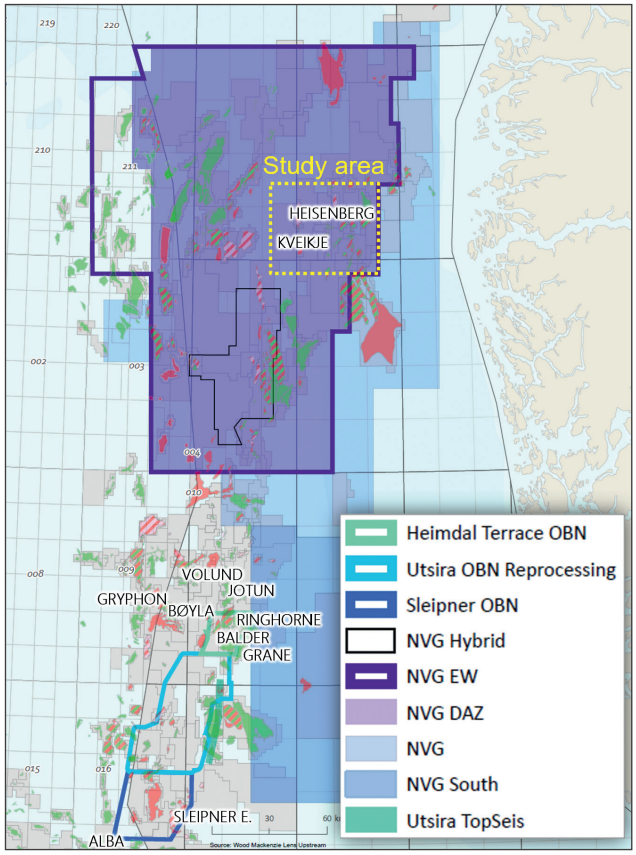

Figure 1 Overview map of the study area indicating the locations of oil and gas fields where sand injectite reservoirs have been documented in the SVG, and where two recent discoveries were made in the NVG area.

Understanding the injectite play

Sand injectites are formed as a result of post-depositional remobilisation and injection of fluidised sands from the 'parent sand' into a mudstone-dominated, potentially sealing, sequence. This process can result in highly permeable reservoirs and can improve both the lateral and vertical connectivity of isolated reservoirs. The injected sands are complex and vary in geometry from being conical-shaped, wing-like, and saucer-shaped to highly irregular complex-shaped intrusions (Huuse et al., 2007). In the North Sea, large-scale sandstone injection complexes are

[1] CGG
* Corresponding author, E-mail: Anna.Rumyantseva@cgg.com
DOI: 10.3997/1365-2397.fb2024038

widespread within fine-grained deepwater mudstone deposits of the late Paleocene-early Eocene sections (Cartwright and Lonergan, 1996). Intrusions can be very thin with steeply dipping flanks, making them difficult to resolve with seismic imaging and evaluate during geological analysis.

The process of injection of fluidised sands typically follows along faults and fractures such as polygonal faults found in the North Sea. These faults are angular in nature and form due to stress variations and dewaterting in low permeable layers. As the sand is injected into these fractures, it can follow the path of least resistance provided by the fault planes. In other cases, the sand injectites cross-cut the polygonal faults and vice versa. This can result in the sand injectites being oriented parallel to the polygonal fault structures. The injectites often become encased within these low-permeability layers as they migrate through the subsurface, as seen in both the Kveikje and Heisenberg discoveries. In Figure 2, the Kveikje complex consists of two reservoir layers of the Late Paleocene-Early Eocene age connected by dyke-shaped injectites. The Heisenberg discovery is shallower in depth with a much stronger amplitude response and is more laterally distributed. Age-equivalent analogues can be seen in the UK North Sea with the Gryphon Field and Fotla discovery, respectively.

In Figure 2, the Kveikje and Heisenberg injectite complexes exhibit variations in the top seismic amplitude response throughout their extent. Well results indicate a gas cap in both discoveries, which we can attempt to correlate to a soft seismic response indicating the possible gas-bearing intervals. To better understand these potential gas-bearing intervals and the complexity of the discoveries, a relative acoustic impedance (AI) attribute is shown in Figure 2b, commonly used to discriminate lithology and thickness variation. This has been obtained by integrating a zero-phase trace and a low-cut Butterworth filter. The Kveikje injectite stands out as low relative AI values rather than a trough-peak pair with zero crossing in the centre of its position observed on the seismic section. This gives us a better estimation of the thickness of the softer sand layer. At the shallower depth of the Heisenberg discovery, the dyke-shaped and concordant sill-shaped injectites stand out as high relative AI features, possibly representing higher-density water-bearing sands compared to low-permeability

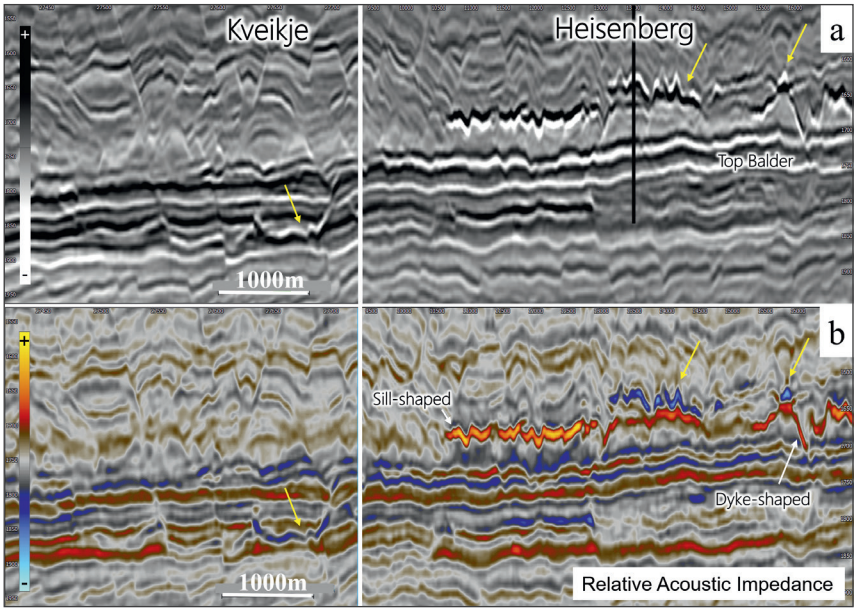

Figure 2 (a) Seismic section through the Kveikje and Heisenberg discoveries; yellow arrows indicate the areas where we observed a soft top of the sand injectites; (b) Relative acoustic impedance attribute section through the Kveikje and Heisenberg discoveries.

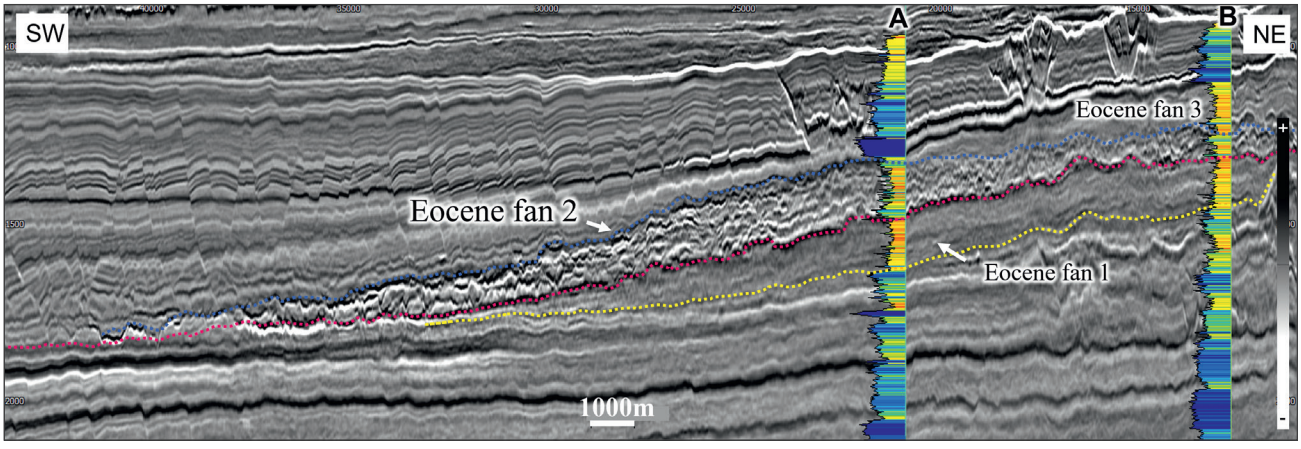

Figure 3 Southwest-Northeast DAZ seismic section passing through Wells A and B; colored gamma-ray wireline log shown at the well locations, which highlights sand intervals in yellow. In the seismic section, the interpreted surfaces correspond to the base (yellow) and top (magenta) of the Eocene fan 1, and the top of the Eocene fan 2 and the base of the Eocene fan 3 indicated in blue.

soft mudstone strata. A clear low relative acoustic impedance is observed at the Heisenberg discovery well location. This is seen where we identify the soft response in the seismic data, which correlates with the presence of the gas cap.

Analysing seismic attributes at the Kveikje and Heisenberg discoveries within the study area makes it possible to identify other injectites that show similar properties and responses. However, before going further, it is essential to establish the context by describing all key elements of the injectite play.

Identifying injectite bodies

To gain a deeper understanding of the complexities of the injectite systems in the study area, it is crucial to identify the sediment supply or the 'parent sand' body. Through our analysis of seismic data and attributes, we can interpret multiple levels of deep marine depositional sand systems. In Figure 3, three sand-rich packages are interpreted within the Eocene interval. A blocky, gamma-ray wireline log (Norwegian Offshore Directorate (NOD) well database) signature through the fans at the locations of Wells A and B indicates thick sandstone units with thin interbeds of mudstones. These sands can be linked to submarine fans originating from the Norwegian mainland which extend into the study area and terminate westwards. They tend to exhibit localised fan depositions that become more channelised basinward.

The base sand unit, Eocene fan 1, consists of low-amplitude, semi-continuous reflections that onlap onto the top boundary of the Balder Formation of Early Eocene age. Eocene fan 2 exhibits a different seismic response, which consists of relatively high-amplitude, partly chaotic internal reflections with discordant high-amplitude anomalies interpreted as sand injectites. The Heisenberg injectite discovery is located at the margin of this fan's western termination. The third sand package, Eocene fan 3, is only present updip and can be seen in Well B. The characteristics of this system are very similar to those of Eocene fan 1 with more conformable, low-frequency reflectivity. This sequence pinches out between Eocene fan 2 and a mud-rich overburden consisting of polygonal faults and injectites. We can observe potential injectite routes from the interaction of these sand packages and mudstone units.

Three types of injectites are identified in the study area, as seen in Figure 4. Type 1 intrusions can be described as conical U, V, and W-shaped intrusions. Type 2 are flat-based bowl or saucer-shaped or wing-like intrusions. Finally, type 3 are irregular or complex sandstone intrusions mostly seen in the Oligocene interval (Nnorom et.al., 2021). The minimum amplitude seismic attribute extracted along horizons at different levels within the Cenozoic seismic units (CSU) illustrates the distribution of injectite complexes and individual injectites as an amplitude anomaly (Rumyantseva et al., 2023). Predominantly, type 1 (mainly V, W and occasionally U-shaped discordant amplitude anomalies) and type 2 (wing-like anomalies) sand injectites can be seen within the Eocene section.

RGB frequency blending from spectral decomposition analysis of an intra Eocene surface, representing the top of Eocene fan 1 and base of Eocene fan 2, illustrates the northeast-southwest direction of sedimentary supply. We see a brighter-frequency

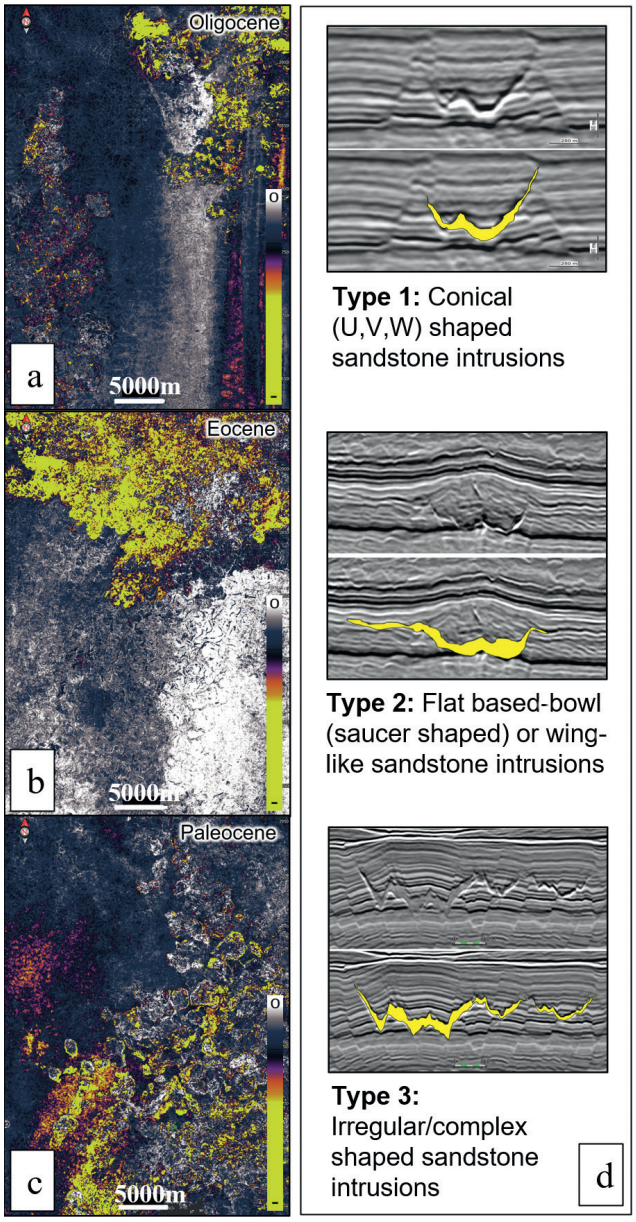

Figure 4 Minimum amplitude seismic attribute extracted along the horizon through the Paleogene sequence showing the distribution of the injectite complexes in the study area: (a) Oligocene interval; (b) Eocene interval; (c) Paleocene interval; (d) seismic sections with different types of injectites identified.

blending response feeding in from the northeast and splaying out to the southwest. Well 35/10-6 confirms the presence of sand at the depth of the analysed surface (Figure 5a). The clear change between the bright, chaotic, undulating area in the north-east and the softer, channel-like frequency response in the central area highlights quite well where the Eocene fan 2 onlaps and pinches out and where the Eocene fan 1 continues to splay out in the central part of the study area.

The sweetness attribute map taken across the fan-splays of Eocene fan 1 shows the high amplitudes indicative of sand variations (Figure 5b). These bright amplitudes correlate with a bright response on the RGB frequency blending (Figure 5a). The seismic section seen in Figure 5c shows the relationship of this unit with the overlying V-shaped or conical type 1 injectites, with concordant sill-shaped elements.

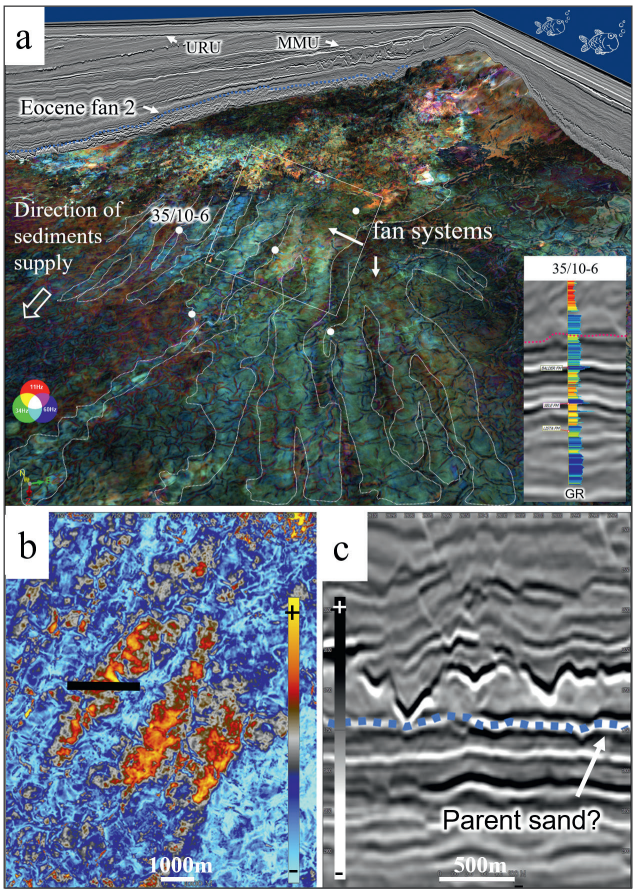

Figure 5 (a) RGB frequency blending from the spectral decomposition analysis of an Intra Eocene surface. Seismic sections in the background of the image illustrate the Eocene fan 2 with highlighted MMU (Mid Miocene Unconformity) and URU (Upper Regional Unconformity). The white dots indicate wells that encountered sandstones at this level; (b) The lateral distribution of the parent sand is illustrated on this sweetness seismic attribute map extracted along the base of the Eocene fan. Black line shows location of the seismic section in image (c); (c) DAZ seismic section through the injectite and possible parent sand.

Identifying injectites and creating geobodies with machine learning

The previously described methods identify the presence of sand injectites but are constrained to the type of display indicating their presence. To fully appreciate their extent and complexity, it is helpful to represent them as 3D geobodies. In-house developed ML tools and the latest DAZ seismic data make this possible to achieve with a much quicker turnaround compared to manually picking the entire 2000 km^2 area.

It is important to have good-quality indicators in the training dataset to ensure the viability of the ML algorithms. The seismic angle stacks were cleaned with deep neural network (DNN) denoise technology, and the time alignment of events was further improved from the near-stack reference point to enhance the amplitude versus offset (AVO). The data was then colour-inverted to Acoustic and Gradient Impedance (AI and GI respectively) and projected into chi values representative of lithology and fluid appropriate for the area.

The initial injectite mask is generated by a customised U-Net model, which has been pre-trained using a realistic synthetic dataset (Sancheti et al., 2023). Different injectite types were accounted for by tailoring this processing to four main areas across the survey, encompassing the variability of size and shape. This preliminary injectite mask and the angle stacks formed the initial training dataset to fine-tune the model, which went through three passes of prediction, retraining, and validation in conjunction with input from in-house geoscientists to reduce erroneous predictions. Their input also proved useful in identifying areas where sampling limitations in the training sets had reduced the effectiveness of the fluid predictions. This was accounted for in later iterations and proved crucial when considering the Heisenberg and Kveikje discoveries.

Throughout these training iterations, the ML was upgraded from 2D training and inference to 3D training, which improved the continuity and reliability of the final injectite mask (Figure 6). Integrating DNN-based workflows into both the processing and interpretation stages of the seismic data analysis helped to obtain results much faster and with more detail (Sancheti et al., 2023). As a result, multiple injectites were created as 'geobodies' using the ML prediction mask. This allowed for a better understanding of the lateral distribution and complex geometries of the injectites (Figure 7). In map view, they vary from circular to oval and are occasionally segmented due to their occurrence within polygonal faults in the host rock.

In addition, a tailored DNN was implemented to assist with fault picking and to help highlight closely spaced polygonal faults in the study areas (Triki et al., 2023). A multi-task 3D UNet model was trained, using realistic noisy synthetic data, to predict both a fault probability and a structurally enhanced seismic volume with a higher signal-to-noise ratio. This approach generated improved fault probabilities with better surface continuity when compared to single-task learning. This was particularly apparent in challenging areas, containing low-resolution seismic events or imbalanced amplitudes within the polygonal faulted complex interval. The probability map predicted via ML was subsequently converted to a fault binary mask based on a user-defined threshold. Figure 8 shows an example of a seismic section and its corresponding fault mask prediction overlaid, both used by an interpreter to individually pick polygonally faulted structures.

To better understand the relationship between the polygonal faults and the injectites, an envelope seismic attribute can be seen in Figure 8e-f. This attribute, known as reflection strength, displays an acoustically strong (bright) response to both negative and positive events. In map view, injectites exhibit polygonal geometries due to their occurrence within polygonally faulted Eocene mudstone host strata. Various interactions between intrusions and fault planes have been observed in the study area. Injectites can be intruded along the fault plane; in other cases, they cross-cut the polygonal faults and vice versa. Additionally, instances have been observed where the propagation of the injectite terminates against a fault plane (Nnorom et al., 2021).

Prospective injectite identification

By analysing the seismic attributes at the location of the Kveikje and Heisenberg discoveries, other injectites of interest can be identified exhibiting similar characteristics and responses. In the map view, Figure 9 focuses on the response seen from the Heisenberg discovery through frequency blending and minimum amplitude results extracted from the upper part of the discovery.

At the Heisenberg discovery location, we observe the distribution of isolated high-amplitude anomalies, with a similar amplitude response in the northwestern corner. Both injectites are situated at the edge of the Eocene basin floor fan. This is where we anticipate facies variations and potential closures often associated with thick sealing mudstone intervals in the flanks of the Eocene fan, which thins westwards. The minimum amplitude extraction made through the potential gas cap shows a similar response in the same injectite to the north-east.

A south-north seismic section (Figure 9c) reveals the identified injectite. It appears disconnected from a larger, brighter injectite to the north. The sandstone reservoir has been injected into the lower-permeability and surrounding polygonal faulted mudstones of the Hordaland Group, creating

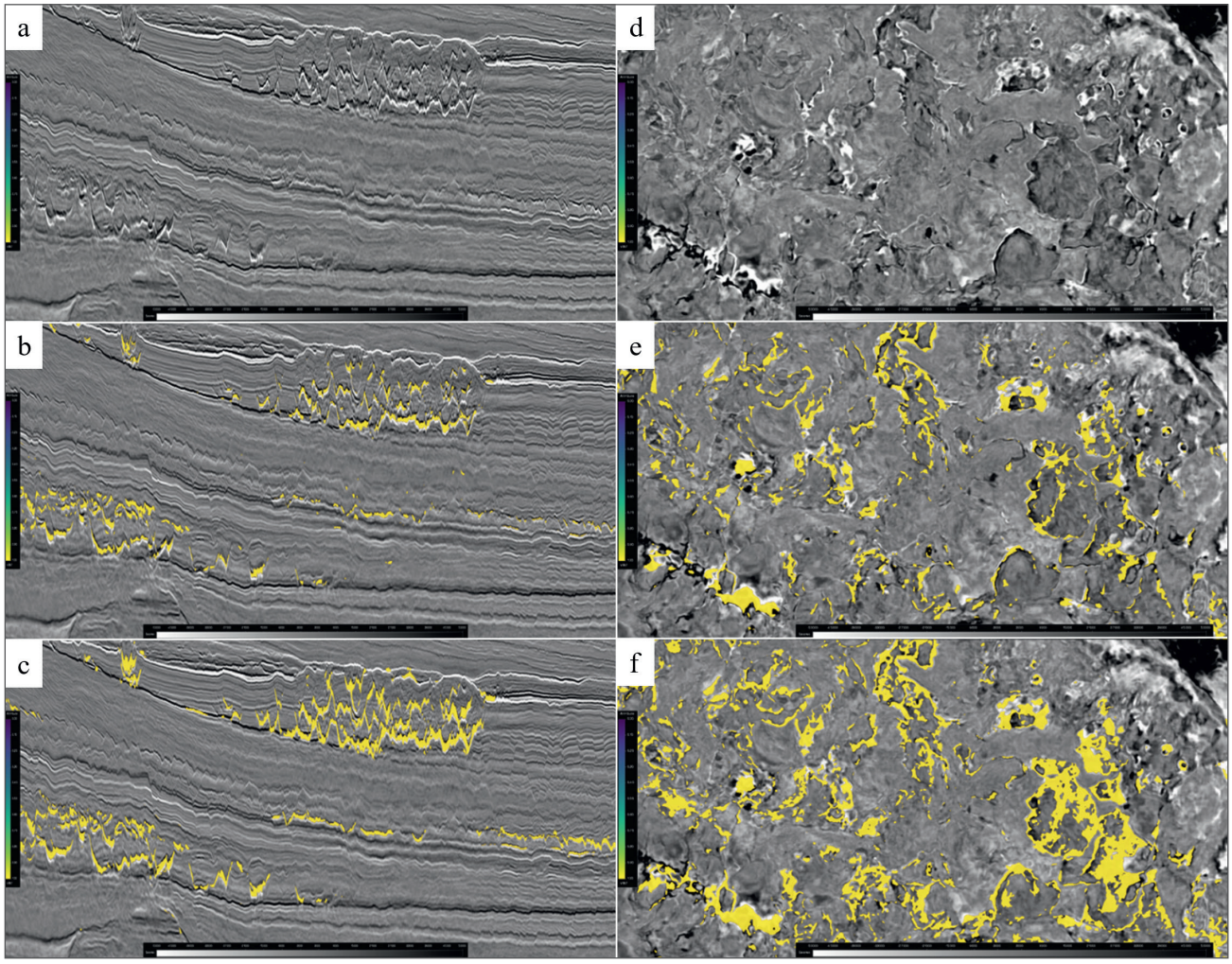

Figure 6 (a) Full stack; (b) Full stack with initial picked injectite mask overlaid; (c) Full stack with final iteration ML 3D injectite mask prediction overlaid; (d) Full stack time slice; (e) Time slice with initial picked injectite mask overlaid; (f) Time slice with final iteration ML 3D mask overlain.

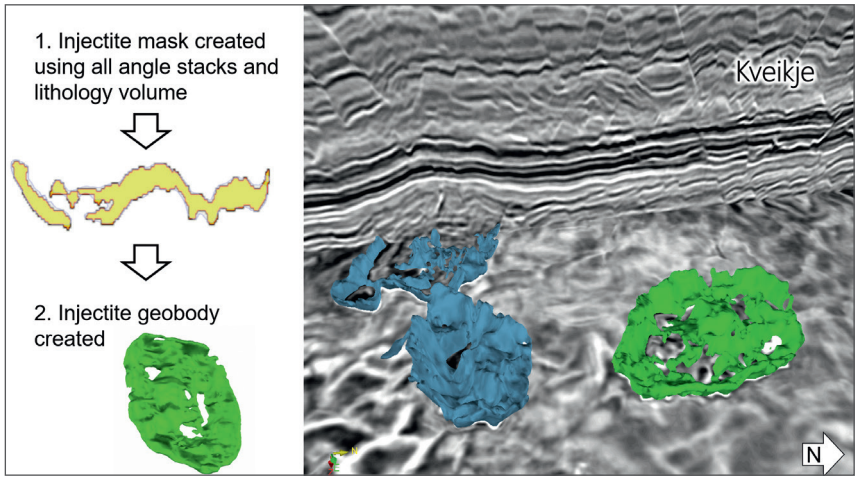

Figure 7 Injectite geobodies extracted from the ML prediction mask. These are conical saucer-shaped in the central part and wing-like types on the sides.

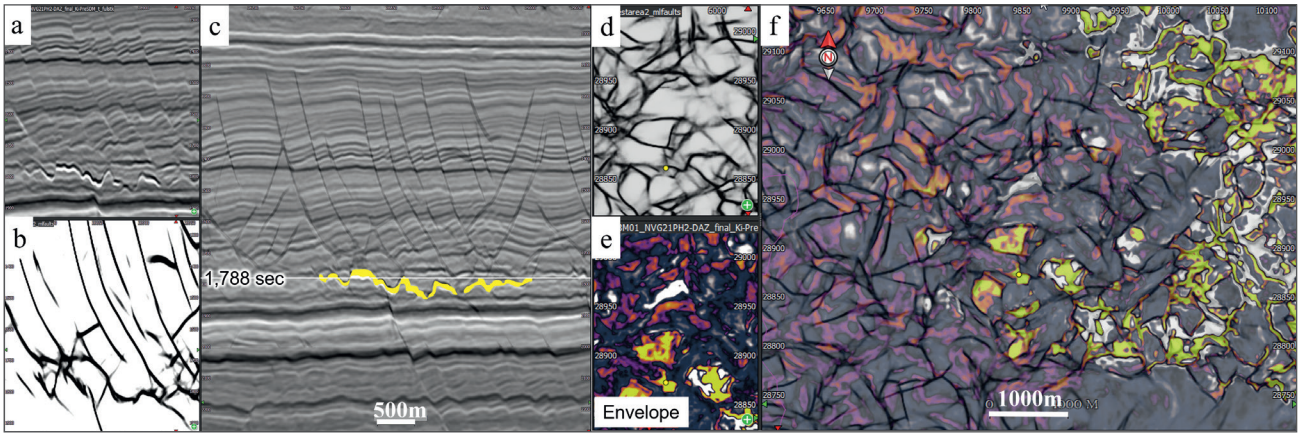

Figure 8 (a) DAZ seismic section; (b) the ML predicted faults; (c) DAZ seismic section with ML fault prediction overlaid and interpreted injectite body shown in yellow; (d) the ML-predicted faults at a 1.788-sec depth; (e) Envelope attribute; (f) Envelope attribute with ML fault delineation overlaid.

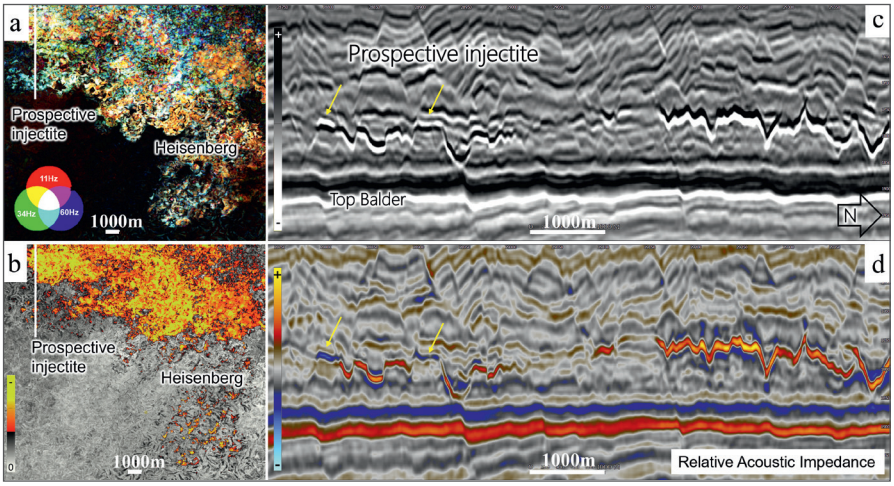

Figure 9 (a) RGB frequency blending from spectral decomposition analysis of an Intra Eocene surface; (b) Minimum amplitude seismic attribute extracted along the horizon at the depth of the Heisenberg discovery; (c) A south-north-oriented seismic section depicting the prospective injectite and the northern injectite complex; (d) Relative acoustic impedance attribute section through the prospective injectite and northern injectite complex.

a potential 'intrusive trap'. Analysing the seismic response seen at Heisenberg as an analogue, we observe both a hard and soft top of the injectite body (soft top highlighted with yellow arrows), where the soft reflector potentially indicates gas-filled parts of the reservoir. On the relative AI section, these parts of the prospective injectite depict lower values, whereas the bright injectite in the north stands out as a continuous sand body with high values (Figure 9d).

These lower relative acoustic impedance values correlate with the strong negative fluid and could indicate gas-filled sandstones (Figure 10a). The fluid attribute was created by combining AI and GI, projecting the data into chi-rotations, and maximising the differences between various fluids. However, it is important to note that brine sands might also contain oil, as oil and brine have similar densities. Therefore, we can suggest that the brine and oil sands are represented in yellow as shown in Figure 10a.

By utilising the ML injectite prediction mask, as described in the previous section, a geobody of the prospective injectite can be created. This extraction allows us to discern the intricate geometry of the feature (Figure 10b). Given the time saved by using the ML-generated injectite mask, we were able to commence the analysis promptly. Furthermore, the lateral distribution of the extracted injectite body is shown in Figure 10c, where we can see the connection of the prospective injectite to the larger body in the west. This sand body can potentially be used for volumetric analysis in subsequent stages.

Conclusions

This study presents a valuable combination of approaches that can be applied to enhance the success rate of sand injectite prediction using seismic attribute analysis and RGB blending combined with DNN algorithms.

The resulting analysis of spectral decomposition and RGB blending allows a better understanding of the deposition pathways of deep marine sediments and the distribution of injectites in the study area. Sweetness, minimum amplitude, envelope, and relative acoustic impedance seismic attributes extracted from the DAZ seismic data provided valuable information about the geophysical properties of the injectites and hosting low-permeability mudstone strata.

Successive iterations of ML training and prediction of the injectites, utilising the seismic data and seismic attribute analysis, honed the results to significantly reduce any erroneous predictions. As a result, several clearly defined geobodies representing the sand intrusives were created. Combining the envelope seismic attribute with ML fault prediction gave a better understanding of the interaction of high-amplitude injectites with the polygonal fault network in the study area.

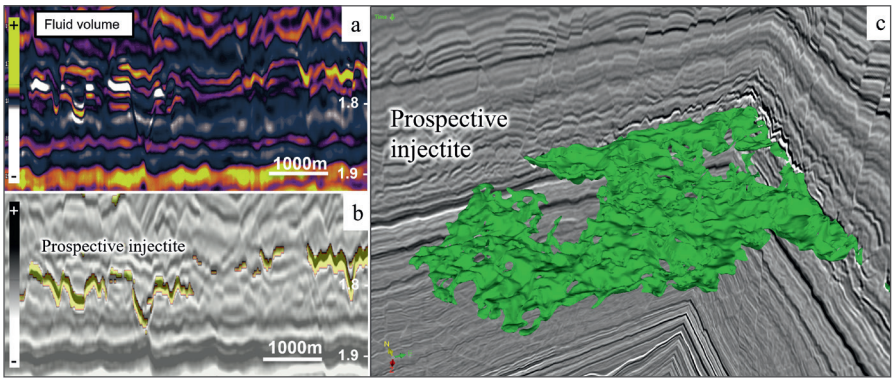

Figure 10 (a) Fluid volume section through the prospective injectite; (b) Seismic section through the injectite with overlaid ML injectite prediction mask shown in yellow; (c) Injectite geobody created from the ML prediction mask.

By comparing seismic attribute responses at the discovery location, we were able to identify other areas with similar properties to the extracted attributes and defined a prospective injectite. The time saved by using the ML-generated injectite mask enabled us to commence the analysis promptly and to create a geobody of the prospective injectite for volumetric analysis.

The proposed methodology has the potential to enhance the success rate of sand injectite prediction in hydrocarbon exploration. In the North Sea there are promising opportunities for near-field accumulations of hydrocarbons. Notably, recent discoveries like Kveikje and Heisenberg serve as excellent examples of this potential.

Acknowledgements

The authors would like to thank CGG Earth Data for permission to show data from the Northern Viking Graben 3D seismic dataset. We acknowledge the contribution made by our colleagues in CGG's Subsurface Imaging and AI Lab teams. Special thanks goes to Professor Mads Huuse for sharing his injectite knowledge with us.

References

Buriola, F., Mann-Kalil, J., Latter, T., Kjølaug, I. and Rumyantseva, A. [2023]. How technological advances in seismic acquisition, processing and imaging can bring new insights to near-field exploration. *First Break*, **41**, 63-70.

Cartwright, J. and Lonergan, L. [1996]. Volumetric contraction during the compaction of mudrocks: A mechanism for the development of regional-scale polygonal fault systems. *Basin Research*, 8, 183-193, https://doi.org/10.1046/j.1365-2117.1996.01536.x.

Huuse, M., Cartwright, J., Hurst, A. and Steinsland, N. [2007]. Seismic Characterization of Large-scale Sandstone Intrusions. Sand injectites: Implications for hydrocarbon exploration and production: *AAPG Memoir,* **87**, 21-35, https://doi.org/10.1306/1209847M873253.

Nnorom, S. and Huuse, M. [2021]. *Three-dimensional seismic and quantitative geometrical characterization of sandstone intrusions in the Paleogene succession of the northern North Sea Basin*; https//pure.manchester.ac.uk/ws/portalfiles/portal/250506344/FULL_TEXT.PDF

Rumyantseva, A., Mann-Kalil, J., Mitchell, S., Macaulay, D. and Sancheti, O. [2023]. New Insights on the Injectite Play in the Northern North Sea using ML; *AAPG ICE conference 2023*, Spain; abstract for poster.

Sancheti, O. and Hou, S. [2023]. *A generalized U-Net for injectite detection*; 84th EAGE Annual Conference Exhibition, abstract.

Triki, A., Latter, T., Hou, S., Raju, A., Bourne, V. and Buriola, F. [2023]. *Using DNNs to overcome challenges in seismic processing and interpretation*; NCS Exploration 2023, abstract.